Desalination and Water Treatment
www.deswater.com

doi: 10.1080/19443994.2016.1186568

57 (2016) 28864–28874
December

Taylor & Francis
Taylor & Francis Group

Adsorption and removal of diethyl phthalate from aqueous media with poly (hydroxyethyl methacrylate) nanobeads

Elif Tümay Özer, Aslı Göçenoğlu Sarıkaya, Bilgen Osman*

Faculty of Science and Art, Uludag University, Görükle Campus, Bursa, Turkey, Tel. +9 0224 2942866; email: etumay@uludag.edu.tr (E. Tümay Özer), Tel. +9 0224 2942863; email: agocenoglu@uludag.edu.tr (A. Göçenoğlu Sarıkaya), Tel. +9 0224 2941735; email: bilgeno@uludag.edu.tr (B. Osman)

Received 21 December 2015; Accepted 30 April 2016

ABSTRACT

In this study, poly (hydroxyethyl methacrylate) (PHEMA) nanobeads with an average size of 115 nm were prepared by emulsion polymerization. The nanobeads were characterized with infrared spectroscopy, scanning electron microscopy, and zeta size analysis. The surface area of the PHEMA nanobeads was calculated as 541.4 m^2/g. Then, diethyl phthalate (DEP) removal efficiency of the PHEMA nanobeads from aqueous media was investigated. At a fixed adsorbent/solution ratio, various factors affecting the adsorption of DEP from aqueous solution such as pH, initial concentration, contact time, temperature, and adsorbent dosage were analyzed. The maximum DEP adsorption capacity of the PHEMA nanobeads was determined as 265.1 mg/g at pH 4.0, 25°C. The Sips isotherm model fits the experimental data in the wide range of DEP concentration tested (1–300 mg/L). The pseudo-first-order, pseudo-second-order, modified Ritchie's-second-order kinetic models were used to test the adsorption kinetics. The DEP adsorption capacity of the nanobeads did not change after five batch successive usages. DEP removal efficiency of the PHEMA nanobeads from different water media such as saliva, sweat, and tap water was also evaluated. The removal efficiencies in the range from 82.4 to 100.0% demonstrate the usability of PHEMA nanobeads for DEP removal from real samples.

Keywords: Diethyl phthalate; Nanobeads; Removal; Adsorption

1. Introduction

Environmental pollution by hazardous organics is one of the most problematic issues worldwide. In addition to the classical priority pollutants (e.g. pesticides), the non regulated so-called emerging contaminants are causing high environmental concern. Emerging contaminants can be broadly defined as any synthetic or naturally occurring chemical or any micro-organism that is not commonly monitored in the environment but has the potential to enter the environment and cause known or suspected adverse ecological and (or) human health effects [1,2]. Phthalic acid esters (PAEs) are present in wastewater, soil, and natural water because of their extensive use in a wide range of applications such as ceramics, toys, paper, medical products, synthetic fibers, cosmetics, and inks, in paint industries, and have become indispensable to our modern society. Large amounts of phthalates leach to the environment by industrial discharge in wastewater and therefore, are suspected as priority

*Corresponding author.

pollutants by the European Environment Agency and US Environmental protection agency [3].

Several number of methods have been used in the removal of PAEs from water including bioconversion [4,5], biodegradation by micro-organisms [6,7] and activated sludge [8,9], advanced oxidation processes [10], and adsorption [3,11–15]. The adsorbents tested for sorption of phthalates were of organic and inorganic origin [11,16–20]. The field of polymer nanoparticles is quickly expanding and playing a pivotal role in a wide spectrum of areas ranging from electronics to photonics, conducting materials to sensors, medicine to biotechnology, pollution control to environmental technology, and so forth, during the past decades [21].

The nanomaterial level is the most advanced at present, both in scientific knowledge and in commercial applications. A decade ago, nanobeads were studied because of their size-dependent physical and chemical properties [22]. Now, they have entered a commercial exploration period [23]. Nanobeads can produce larger specific surface area and, therefore, may result in high binding capacity. Many published works focused on the synthesis of micrometer-sized polymer matrix. Only limited work has been published on the application of nanobeads in the adsorption of PAEs. Graphene [24] and graphene oxide-functionalized magnetic nanoparticles [25], chloromethylated polystyrene magnetic nanospheres [26], magnetic multi-walled carbon nanotubes [27] were used for enrichment of PAEs in different matrices.

The main objective of this study is to report the synthesis of poly (hydroxylethyl methacrylate) (PHEMA) nanobeads and their use in the adsorptive removal of DEP from aqueous solution. PHEMA nanobeads were produced by emulsion polymerization technique. Then, the PHEMA nanobeads were characterized by scanning electron microscopy (SEM), infrared spectroscopy (IR), and zeta size analyses. Removal studies were conducted to evaluate the binding capacity of DEP onto the PHEMA nanobeads. In order to clarify the adsorption process, adsorption isotherms and kinetic studies were conducted. PHEMA nanobeads were also used to remove DEP from artificial saliva, sweat, and tap water.

2. Experimental

2.1. Chemicals

Diethyl phthalate (DEP) was purchased from Merck (Darmstadt, Germany). Ethylene glycol dimethacrylate (EGDMA) was obtained from Merck (Darmstadt, Germany), purified by passing through active alumina, and stored at 4°C until used. Sodium dodecyl sulfate (SDS) and hydroxyethyl methacrylate (HEMA) were obtained from Merck (Darmstadt, Germany). Polyvinyl alcohol (PVA; Mw: 100,000, 98% hydrolyzed) was supplied by Aldrich Chem. Co., (USA). All other chemicals were of reagent grade and were purchased from Merck AG (Darmstadt, Germany). All water used in the binding experiments was purified using a Barnstead (Dubuque, IA) ROpureLPw reverse osmosis unit with a high-flow cellulose acetate membrane (Barnstead D2731), followed by a Barnstead D3804 NANOpurew organic/colloid removal and ion-exchange packed-bed system.

2.2. Synthesis of PHEMA nanobeads

PHEMA nanobeads were prepared using emulsion polymerization method as given below. Firstly, two aqueous phases and oil phase were prepared. The first aqueous phase is composed of 93.8 mg PVA, 14.43 mg SDS, and 11.73 mg $NaHCO_3$ in 5 mL water. For the second aqueous phase, 50 mg PVA and 50 mg SDS were dissolved in 100 mL water. To prepare oil phase, HEMA and EGDMA were mixed and added to the first aqueous phase to obtain a mini-emulsion. Then, the mixture was homogenized at 25,000 rpm (IKA, T25 digital ULTRATURRAX). The prepared mini-emulsion was added to the second aqueous phase followed by the addition of 57.5 mg $NaHSO_3$ and 63 mg ammonium persulphate (APS). Polymerization was performed at 40°C for 6 h and was also verified with the occurrence of white colour of medium. After completion of the polymerization, nanobeads were cleaned by washing with ethanol and water several times to remove the unreacted monomers. For this purpose, the nanobeads were precipitated and collected with the help of a centrifuge (Allegra 64R, Beckman Coulter) at 61,000 g for 1 h and resuspended in ethanol and water several times. After that, PHEMA nanobeads were further washed with deionized water. Finally, nanobeads were stored in water as a suspension. The amount of nanobeads in solution (mg nanobeads/mL solution) was determined by evaporating 1 mL of solution in drying oven.

2.3. Characterization studies

IR analysis of PHEMA nanobeads was performed using FTIR spectrophotometer (Perkin Elmer, Spectrum 100, USA).

The average nanobead size and size distribution were determined by Zeta Sizer (Malvern Instruments, Model 3000 HSA, England).

The morphology of the PHEMA nanobeads was observed via a scanning electron microscope (SEM) (Jeol, JEM 1200EX, Tokyo, Japan).

2.4. Batch adsorption experiments

Batch analysis was used for the determination of adsorption isotherms for DEP adsorption on PHEMA nanobeads. Nanobeads were added into eppendorf tubes (1 mL) containing DEP solutions at 25°C and different pH. The equilibrium was maintained in Eppendorf tubes kept in a rotator (Medispec) at a constant speed (25 rpm). Then, the adsorption systems were centrifuged at 14,000 rpm and DEP concentrations in the supernatant were determined spectrophotometrically (239 nm). The amount of adsorbed DEP was calculated as:

$$Q = \frac{[(C_0 - C)V]}{m} \quad (1)$$

where Q is the amount of adsorbed DEP on a unit mass of the beads (mg/g); C_0 and C are the concentrations of DEP in the initial solution and in the aqueous phase after treatment for a certain period of time, respectively (mg/L); V is the volume of the aqueous phase (mL); and m is the mass of the PHEMA nanobeads used (g).

The initial concentration of DEP in the aqueous phase was determined using calibration plot obtained with pure DEP solutions at different concentrations. The measurements were performed spectrophotometrically at 239 nm.

The influence of the pH on DEP adsorption on PHEMA nanobeads was studied by adjusting aqueous phase to different initial pH values from 2 to 10. The initial concentration of DEP was 20 mg/L. The pH was adjusted using 0.1 M HCl and 0.1 M NaOH solutions.

In order to investigate the effect of initial DEP concentration on the adsorption capacity of PHEMA nanobeads, the concentration of DEP in the medium was varied in the range of 1–300 mg/L at pH 4.0.

2.5. Removal of DEP from different matrices

To evaluate the effectiveness of PHEMA nanobeads for DEP removal from different media, saliva, sweat, and tap water samples were used. About 5 ppm DEP solution was spiked to 1 mL of saliva, sweat, and tap water samples. And then, different amounts of PHEMA nanobeads (0.53–2.65 mg) were added to solutions and recovery values were calculated. For each sample, three replicate experiments were performed.

Artificial saliva was prepared by dissolving 0.17 g of $MgCl_2{\cdot}6H_2O$, 0.15 g of $CaCl_2{\cdot}6H_2O$, 0.76 g of $K_2HPO_4{\cdot}2H_2O$, 0.53 g of K_2CO_3, 0.33 g of NaCl, and 0.75 g of KCl (analytical-reagent grade, Merck) in 1 L of water and the solution pH was adjusted to 6.8 ± 0.1 with 1% HCl (DIN V 53160-1).

Artificial sweat was prepared by dissolving 5.0 g of NaCl, 1.0 g of urea, and 1.0 g of lactic acid (analytical-reagent grade, Merck) in 1 L of water and the solution pH was adjusted to 6.5 ± 0.1 with 1% NH_3 (DIN V 53160-2).

2.6. Desorption of DEP from PHEMA nanobeads and reusability

In order to determine the reusability of PHEMA nanobeads, the DEP adsorption and desorption cycle was repeated five times using the same nanobeads (initial DEP concentration: 20 mg/L). The DEP desorption from the PHEMA nanobeads was carried out with a methanol–acetic acid (9:1 v/v) solution by stirring magnetically at 150 rpm at room temperature for 3 h. The beads were separated from desorption medium by centrifuging (Beckman Coulter, Allegra 64R Centrifuge) at 15,000 rpm for 30 min. The supernatant was removed and used for determining desorption amount of DEP. The beads were washed with excess amount of water several times followed by centrifugation. The same beads were used for DEP adsorption.

3. Results and discussion

3.1. Characterization of the PHEMA nanobeads

Nanobeads have larger surface area and therefore may result in high adsorption capacity. Therefore, it may be advantageous to synthesize nanobeads with large surface area and utilize them as suitable carriers for the adsorption The surface area of the PHEMA nanobeads was calculated using the following expression:

$$N = \frac{6.10^{10}.S}{\pi.\ \rho_x.\ d^3} \quad (2)$$

where N is the number of nanobeads per milliliter; S is the % of solids; ρ_x is the density of bulk polymer

(g/mL); and d is the nanobead diameter (nm). The number of nanobeads in mL suspension was determined by utilizing from mass-volume graph of nanobeads. From all these data, specific surface area of the PHEMA nanobeads was calculated by multiplying N and surface area of one nanobead. The specific surface area was calculated as 541.4 m^2/g PHEMA nanobeads. It can be clearly seen that the PHEMA nanobeads are perfectly spherical with a smooth surface as shown by the scanning electron (SEM) microscopy image (Fig. 1). Emulsion polymerization provided PHEMA nanobeads with an average size of 115 nm and a polydispersity index of 0.196 (Fig. SI1). Polydispersity index is an indicator of aggregation in the nanoparticles. The lower the polydispersity index, the lower the tendency to aggregate. The low polydispersity index of PHEMA nanobeads demonstrates the dispersivity in water. The existence of hydroxyl group on the surface of the PHEMA nanobeads also increases the dispersivity in water by ultrasonication. The aqueous dispersion of nanobeads was stable for several days.

FTIR spectrum of PHEMA is shown in Fig. 2. The n(O–H) stretching vibration in PHEMA is observed in the 3,250–3,500 cm^{-1} as a broad absorption band, indicated a strong band at 1,716 cm^{-1} due to n(C=O) group and the 2,948 cm^{-1} n(C–H) stretching of CH_3, the 1,268 cm^{-1} n(C–O) stretching vibration.

3.2. Effect of pH on DEP adsorption

One of the most important parameters affecting the adsorption capacity is pH of solution. Because the solution pH could change both the existing form of the target compound and the charges on the adsorbent surface. Fig. 3 shows the effect of solution pH on the amount of adsorbed DEP with PHEMA nanobeads. The hydroxyl (OH) group in the PHEMA nanobeads acts as a proton donor. The main interaction is hydrogen bond formed between hydroxyl group of PHEMA and carbonyl group (C=O) of DEP molecule, which acts as a proton acceptor. The hydroxyl group of HEMA has high pK_a value (13.82) and so that the acidity of the OH group is low. The OH groups of PHEMA act as proton donor in the pH range of 2–10. The possible interaction between PHEMA nanobeads and DEP molecules was depicted in Fig. 4. As a result, the adsorption capacity of the PHEMA nanobeads hardly varied over the whole pH range of 2–10. The characteristic feature of the PHEMA nanobeads can be applicable in real samples without the need to adjust pH.

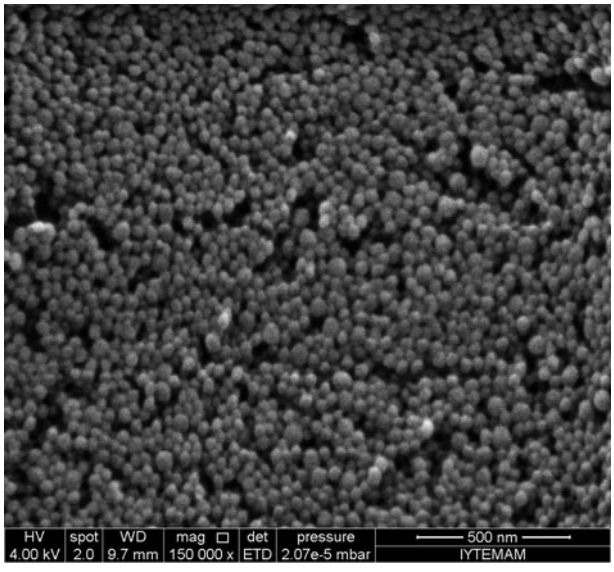

Fig. 1. SEM image of PHEMA nanobeads.

3.3. Kinetic studies

Kinetic studies were conducted at three different temperatures (4, 25, and 45°C) at 20 mg/L initial concentration of DEP. The decrease in DEP adsorption with the increase in temperature from 4 to 45°C shows that the adsorption is exothermic. As shown in Fig. 5, for all tested temperatures, adsorption rates were extremely fast. The result shows that the PHEMA nanobeads can be effectively used to separate DEP from aqueous medium. For testing the dynamic experimental data, pseudo-first-order kinetic model, pseudo-second-order kinetic model, modified Ritchie's-second-order kinetic model were used at the initial concentration, 20 mg/L of DEP and three temperatures (298, 308, and 318 K) for 180 min at pH 4.0.

The linear form of the applied model can be given as:

$$\text{Pseudo-first-order:}\quad \log(q_e - q_t) = \log\, q_e - \frac{k_1 t}{2.303} \tag{3}$$

$$\text{Pseudo-second-order:}\quad \frac{t}{q_t} = \frac{1}{k_2 q_e^2} + \frac{1}{q_e} t \tag{4}$$

$$\text{Modified Ritchie's-second-order:}\quad \frac{1}{q_t} = \frac{1}{k_R q_e t} + \frac{1}{q_e} \tag{5}$$

where k_1 (1/min), k_2 ((g/mg)/min), and k_R (1/min) are kinetic constants for pseudo-first-order, pseudo-second-order and Modified Ritchie's-second-order kinetic models, respectively. q_e and q_t (mg/g) are the amounts of the DEP adsorbed at equilibrium and at

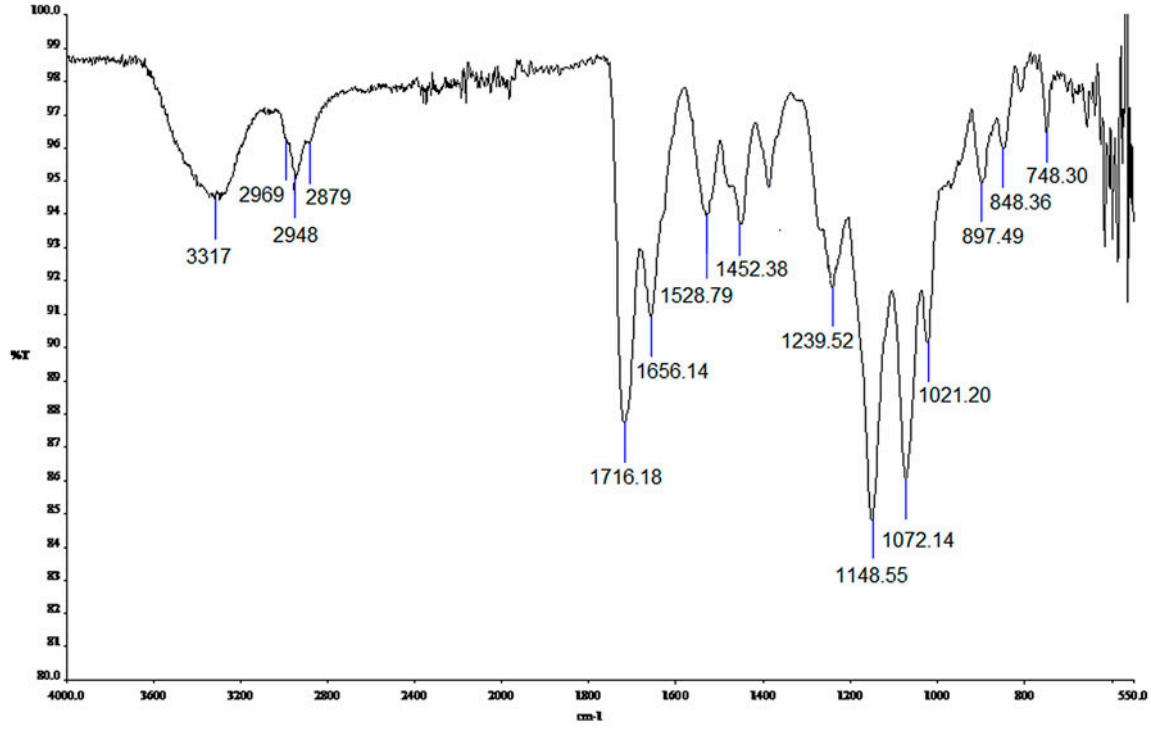

Fig. 2. FTIR spectrum of PHEMA nanobeads.

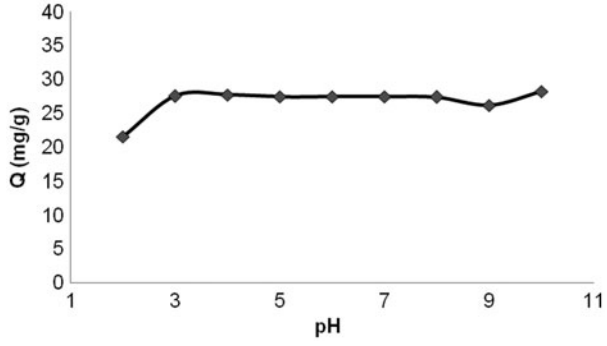

Fig. 3. Effect of solution pH on the amount of adsorbed DEP with PHEMA nanobeads.

time (min), respectively. The values of constants in Eqs. (3)–(5) can be obtained from the slopes and intercepts of the fitted curves.

The validities of these three kinetic models for all temperatures were checked and the values of the parameters and correlation coefficients obtained from these three kinetic models are all listed in Table 1. The correlation coefficients of pseudo-second-order model greater than 0.9995 (R^2) for all temperatures and also the q_e values close to the experimental q_e values for all temperatures indicated the second-order nature of the present adsorption process.

3.4. Adsorption isotherms

The adsorption behavior of the PHEMA nanobeads was also investigated. Adsorption isotherms were studied at the concentration of 7.6 mg/mL PHEMA nanobeads with the concentrations of the DEP being varied in the range from 1.0 to 300 mg/L at pH:4.0, 25℃ (Fig. 6). The maximum DEP adsorption capacity of the PHEMA nanobeads was determined as 265.1 mg/g at pH 4.0, 25℃. The DEP adsorption capacity of PHEMA nanobeads were compared with some reported adsorbents [16,20,25,28–32] and shown in Table 2.

In order to quantitatively describe the adsorption capacity of the PHEMA nanobeads, firstly, commonly used adsorption isotherms, the Langmuir and the Freundlich, were applied to the experimental data. The Langmuir adsorption isotherm model explains the variation in adsorption of molecules (adsorbates) with pressure. The isotherm is based on the assumption that maximum adsorption occurs when a saturated monolayer of adsorbate molecules is present on the adsorbent surface, the energy of adsorption is

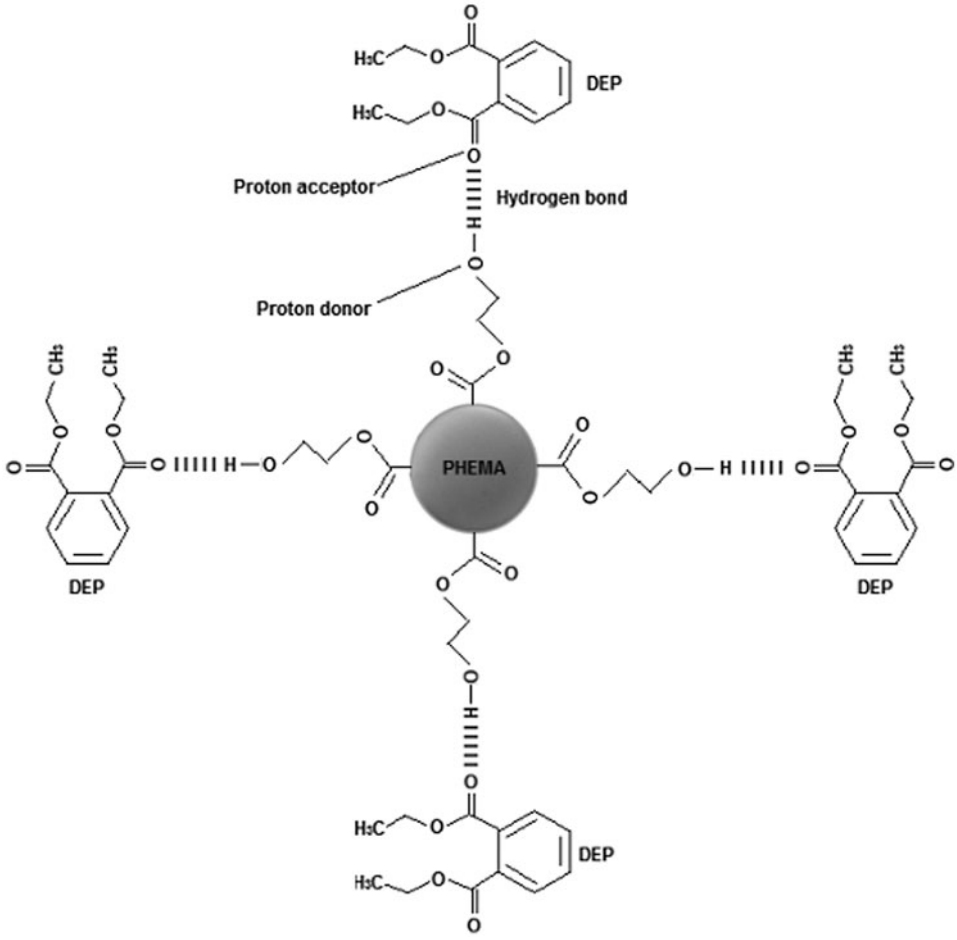

Fig. 4. The interaction between PHEMA nanobeads and DEP molecules.

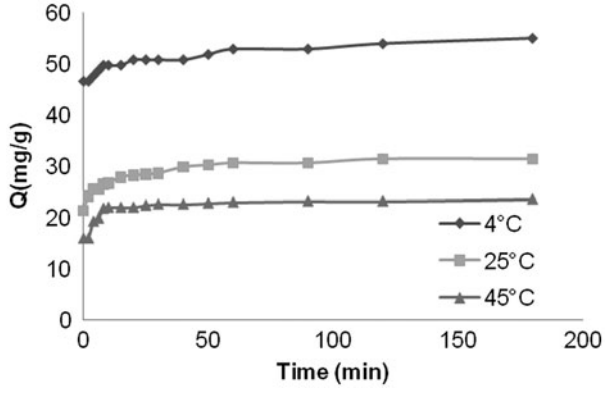

Fig. 5. Effect of contact time and temperature on the amount of adsorbed DEP PHEMA (initial DEP concentration: 20 mg/L, pH 4.0).

constant, and there is no migration or interaction between the adsorbate molecules in the surface plane [33,34]. The Freundlich isotherm explains that the extent of adsorption varies directly with pressure. This empirical relationship describes the multilayer adsorption of heterogeneous systems and assumes that different sites share several adsorption energies involved [35].

The Langmuir adsorption equations are expressed in Eq. (6):

$$\frac{C_e}{q_e} = \frac{1}{Q_L K_L} + \frac{C_e}{Q_L} \tag{6}$$

and the Freundlich model equation is expressed in Eq. (7):

$$\ln q_e = \ln K_F + \frac{1}{n} \ln C_e \tag{7}$$

where Q_L is the maximum adsorption at monolayer coverage (mg/g), q_e is the DEP concentration on the

Table 1
Kinetic parameters for the adsorption of DEP onto the PHEMA nanobeads

Parameters	Experimental	Pseudo-first-order kinetic model			Pseudo-second-order kinetic model			Modified Ritchie's-second order kinetic		
Temperature (K)	q_e (mg/g)	$k_1 \times 10^2$ (1/min)	q_{eq} (mg/g)	R^2	$k_2 \times 10^2$ ((g/mg)/min)	q_{eq} (mg/g)	R^2	k_R (1/min)	q_{eq} (mg/g)	R^2
277	55.03	1.38	6.97	0.9305	1.12	55.56	0.9995	3.80	52.63	0.7063
298	31.38	2.76	6.44	0.9062	1.58	32.26	0.9998	1.74	30.30	0.7577
318	23.59	2.99	3.59	0.7547	3.46	23.81	0.9999	1.10	23.81	0.9793

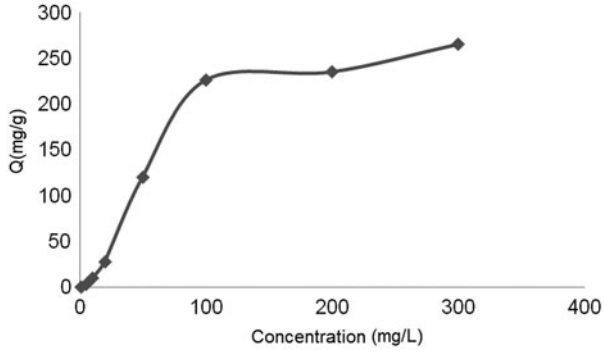

Fig. 6. Effect of DEP concentration on the amount of adsorbed DEP with PHEMA nanobeads (pH 4.0, T: 25°C).

PHEMA nanobeads at equilibrium (mg/g), C_e denotes the concentration of the DEP in solution at equilibrium (mg/L), K_L is the Langmuir adsorption equilibrium constant (L/mg), reflecting the energy of the adsorption, K_F and $1/n$ are the Freundlich characteristic constants, indicating the adsorption capacity and the adsorption intensity, respectively. The values of K_L and Q_L can be obtained from the intercept and slope of the linear plot of C_e/q_e vs. C_e and the values of K_F and $1/n$ can be obtained from the intercept and slope of the linear plot of ln q_e vs. ln C_e, respectively.

The results shown in Table 3 indicate that the adsorption of DEP onto PHEMA nanobeads did not comply with both the Langmuir and the Freundlich isotherm models in the wide range of DEP concentration tested. However, the Langmuir and Freundlich models fit well with high correlation coefficients at high initial DEP concentration (100–300 mg/L, $R^2 = 0.9885$) and at low initial DEP concentration (1–100 mg/L, $R^2 = 0.9942$), respectively. The Q_L and K_L values for the adsorption of DEP by the nanobeads calculated from the Langmuir isotherm model were 294.1 mg/g and 0.0285 L/mg, respectively. The $1/n$ and K_F values for the adsorption of DEP by the nanobeads calculated from the Freundlich isotherm model were 1.5554 and 0.237 (mg/g)(L/mg)$^{1/n}$.

The Sips isotherm model (the Langmuir–Freundlich isotherm model) derived from the limiting behavior of the Langmuir and Freundlich isotherms [36] was also used to test experimental data. When C_e approaches a low value, the Sips isotherm effectively reduces to Freundlich, while at high C_e, it predicts the Langmuir monolayer sorption characteristic. The Sips linear model is expressed as:

$$\frac{1}{q_e} = \frac{1}{Q_{max} K_s} \left(\frac{1}{C_e}\right)^{1/n} + \frac{1}{Q_{max}} \tag{8}$$

Table 2
Comparison of DEP adsorption capacity for different adsorbents

Adsorbent	Q (mg DEP/g adsorbent)	Optimum pH	Equilibrium time	Refs.
Chitosan bead	0.19	8.0	6 h	[28]
Molybdate-impregnated chitosan bead	2.64	6.0–9.0	6 h	[29]
α-Cyclodextrin-linked chitosan bead	2.82	6.0–9.0	6 h	[30]
Magnetic poly(EGDMA-VP) bead	98.9	3.0–10.0	3 h	[16]
Graphene-MNPs	–	2.0–10.0	15 min	[31]
Nylon6 nanofibers	–	7.0	12.5 min	[32]
GO-MNPs	8.71	3.0–10.0	5 min	[25]
Poly(EGDMA-MATrp) beads	590.7	2.0–10.0	50 min	[20]
This study	265.1	3.0–10	15 min	–

Table 3
Parameters of Langmuir, Freundlich, and Sips isotherm models for the adsorption DEP onto the PHEMA nanobeads

Parameters	Langmuir isotherm constants (100–300 mg/L)			Freundlich isotherm constants (1–100 mg/L)			Sips isotherm constants (1–300 mg/L)		
Temperature (K)	$K_L \times 10^2$ (L/mg)	Q_L (mg/g)	R^2	K_F (mg/g) (L/mg)	n	R^2	$K_s \times 10^2$ (L/mg)	Q_{max} (mg/g)	R^2
298	2.85	294.1	0.9886	0.237	0.643	0.9942	1.60	256.4	0.9996

where K_s (L/mg) and Q_{max} (mg/g) are the Sips equilibrium constant and maximum adsorption capacity values obtained from the slope and intercept of the plot.

In the analysis of the Langmuir, the Freundlich and the Sips equations applied to the experimental data, one possible interpretation is that there are two types of binding, as follows:

(1) In low solution concentration (1–100 mg/L), the Freundlich isotherm fits the experimental data. Therefore, PHEMA nanobeads have different binding sites have several adsorption energies involved. Adsorption process is multilayer adsorption. The Freundlich isotherm model, historically developed for the adsorption of animal charcoal, demonstrates that the ratio of the adsorbate onto a given mass of adsorbent to the solute was not a constant at different solution concentrations [37]. The SEM analysis of the PHEMA nanobeads shows that the nanobeads are approximately 50 nm in diameter. However, the average size of the PHEMA nanobeads was determined as 115 nm in diameter. As a conclusion, the PHEMA nanobeads aggregate noticeably in aqueous solution. In this perspective, the amount adsorbed is the summation of adsorption on all sites, with the stronger binding sites are occupied first, until adsorption energy are exponentially decreased upon the completion of adsorption process [38].
(2) In high solution concentration (100–300 mg/L), inversely the multilayer adsorption in low solution concentration, the adsorption proceeds according to the Langmuir isotherm model. Firstly, the heterogeneous binding sites on PHEMA nanobeads were occupied with DEP molecules in solution. Then, the residual DEP molecules bind to the adsorbed DEP molecules via weaker van der Waals interactions. This adsorption process is monolayer adsorption and it can be described by the Langmuir model. Therefore, the Sips isotherm model derived from the limiting behavior of the Langmuir and Freundlich isotherms fits well the experimental data with high correlation efficient ($R^2 = 0.9996$) in the wide range of DEP concentration tested (1–300 mg/L). The K_s and Q_{max} values were determined as 0.016 L/mg and 256.4 mg/g (Table 3). The high correlation coefficient and the Q_{max} value approximate to the experimental q_e value determined for DEP adsorption supports the adsorption process explained above.

3.5. Effect of the amount of nanobeads for different water media

In order to choose the optimum amount of the adsorbent for the adsorption of DEP, the adsorbed amounts of DEP on PHEMA nanobeads were investigated using different amount of PHEMA nanobeads ranging from 0.53 to 2.65 mg. The effect of the amount of nanobeads on DEP adsorption was investigated in different media such as saliva, sweat, and tap water. The removal efficiencies depicted in Fig. 7 show that the adsorption of DEP could reach the maximum plateau when the amount of PHEMA nanobeads was increased to 2.65 mg for all matrices. The removal efficiencies for DEP in artificial saliva, sweat, and tap water samples fell in the range from 82.4 to 100.0% and the repeatabilities expressed as the relative standard deviations (RSDs) varied from 0.2 to 5.3%. The removal efficiency is highest in artificial sweat samples for all studied PHEMA nanobead amounts due to the increase in weak van der Waals interactions via sample salinity. As a whole, the recoveries of spiked water samples are very satisfactory. In addition, independence of the adsorption amount of DEP onto PHEMA nanobeads from pH enables the removal of DEP from different water media without the need to adjust pH. These advantages of PHEMA nanobeads can be practicable in real water samples.

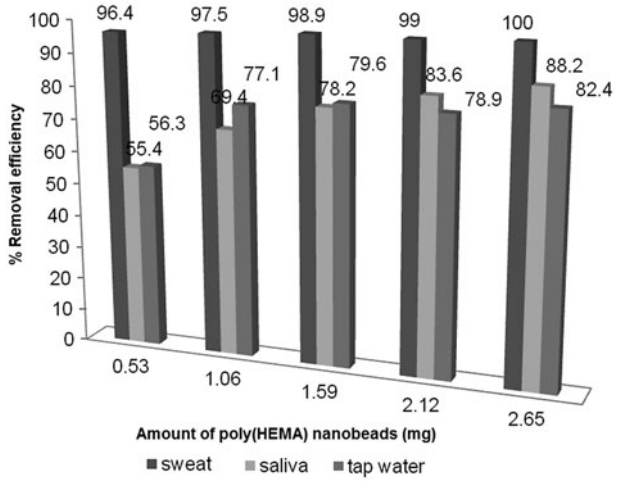

Fig. 7. Removal efficiencies of DEP in different matrices with different amount of PHEMA nanobeads.

3.6. Desorption of DEP from PHEMA nanobeads

Desorption of DEP from PHEMA nanobeads was carried out in a batch system (initial DEP concentration: 20 mg/L). The DEP adsorption capacity did not change during five successive adsorption–desorption cycles (28.1, 27.6, 28.0, 28.2, and 27.4 mg/g polymer). These results showed that PHEMA nanobeads can be repeatedly used in DEP adsorption without excessive losses in their initial adsorption capacity.

4. Conclusions

In this research, PHEMA nanobeads were produced by emulsion polymerization. The prepared nanobeads were characterized and used as an effective adsorbent for the removal of DEP in water, artificial saliva, and sweat samples for the first time. Firstly, the adsorption process of DEP onto PHEMA nanobeads was clarified with isotherm and kinetic studies. The application of two isotherm models generally showed that a single Langmuir or Freundlich equation cannot fit the entire concentration gap. This indicates that DEP adsorption probably occurred via two adsorption mechanisms (multilayer and monolayer adsorptions). The adsorption process could be best described by the pseudo-second-order kinetic model. The total capacity of PHEMA nanobeads was determined as to be 265.1 mg/g at pH 4.0, 25°C. The nanobeads can be regenerated easily without loses in initial adsorption capacity. The results obtained for different water media such as saliva, sweat, and tap water indicated that PHEMA nanobeads could be a promising adsorbent for solid-phase extraction with great application potentials.

Supplementary material

The supplementary material for this paper is available online at http://dx.doi.10.1080/19443994.2016.1186568.

Acknowledgements

This work was supported by the Research Foundation of Uludağ University Project Number: KUAP(F)-2013/86.

Abbreviations

ρ_x	—	the density of bulk polymer (g/mL)
$1/n$	—	the Freundlich constant indicating the adsorption intensity
C_0	—	initial concentration of DEP in solution (mg/L)
C_e	—	concentration of DEP at equilibrium (mg/L)
d	—	the nanobead diameter (nm)
k_1	—	the kinetic constant of pseudo-first-order kinetic model (1/min)
k_2	—	the kinetic constant of pseudo-second-order kinetic model ((g/mg)/min)
K_F	—	the Freundlich constant indicating the adsorption capacity ((mg/g) $(L/mg)^{1/n}$)
K_L	—	the Langmuir adsorption equilibrium constant (L/mg)
K_R	—	the kinetic constant of Modified Ritchie's-second-order kinetic model (1/min)
K_s	—	the Sips equilibrium constant (L/mg)
m	—	the mass of the nanobeads used (g)
Q	—	the amount of adsorbed DEP on a unit mass of the beads (mg/g)
q_e	—	the amount of DEP adsorbed at equilibrium (mg/g)
Q_L	—	the maximum amount of DEP adsorbed per unit mass adsorbent (mg/g)
Q_{max}	—	maximum adsorption capacity (mg/g)
q_t	—	the amount of DEP adsorbed at any time (mg/g)
R^2	—	linear regression coefficient
S	—	the % of solids
T	—	temperature (K)
t	—	time (min)
V	—	the volume of the aqueous phase (mL)

References

[1] M. Kuster, M.J.L. López de Alda, M.D. Hernando, M. Petrovic, J. Martín-Alonso, D. Barceló, Analysis and occurrence of pharmaceuticals, estrogens, progestogens and polar pesticides in sewage treatment plant effluents, river water and drinking water in the Llobregat river basin (Barcelona, Spain), J. Hydrol. 358 (2008) 112–123.

[2] S.D. Richardson, T.A. Ternes, Water analysis: Emerging contaminants and current issues, Anal. Chem. 83 (2011) 4614–4648.
[3] N.A. Khan, B.K. Jung, Z. Hasan, S.H. Jhung, Adsorption and removal of phthalic acid and diethyl phthalate from water with zeolitic imidazolate and metal–organic frameworks, J. Hazard. Mater. 282 (2015) 194–200.
[4] J. Ejlertsson, M. Alnervik, S. Jonsson, B. Svensson, Influence of water solubility, side-chain degradability, and side-chain structure on the degradation of phthalic acid esters under methanogenic conditions, Environ. Sci. Technol. 31 (1997) 2761–2764.
[5] R. Iturbe, G. Moreno, P. Elefsiniotis, Efficiency of a phthalate ester in an activated-sludge system, Environ. Technol. 12 (1991) 783–796.
[6] D. Sompornpailin, S. Siripattanakul-Ratpukdi, A.S. Vangnai, Diethyl phthalate degradation by the freeze-dried, entrapped Bacillus subtilis strain 3C3, Int. Biodeterior. Biodegrad. 91 (2014) 138–147.
[7] Z.D. Wen, D.W. Gao, W.M. Wu, Biodegradation and kinetic analysis of phthalates by an Arthrobacter strain isolated from constructed wetland soil, Appl. Microbiol. Biotechnol. 98 (2014) 4683–4690.
[8] D.L. Wu, B.L. Hu, P. Zheng, M. Qaisar, Anoxic biodegradation of dimethyl phthalate (DMP) by activated sludge cultures under nitrate-reducing conditions, J. Environ. Manage. 19(10) (2007) 1252–1256.
[9] H.F. Cheng, M. Kumar, J.G. Lin, Assessment of di-(2-ethylhexyl)phthalate (DEHP) removal in a rotating biological contactor and activated sludge process treating domestic wastewater, Sep. Sci. Technol. 45(2) (2010) 221–227.
[10] M.M. Abdel daiem, J. Rivera-Utrilla, R. Ocampo-Pérez, J.D. Méndez-Díaz, M. Sánchez-Polo, Environmental impact of phthalic acid esters and their removal from water and sediments by different technologies—A review, J. Environ. Manage. 109 (2012) 164–178.
[11] E. Ayranci, E. Bayram, Adsorption of phthalic acid and its esters onto high-area activated carbon-cloth studied by *in situ* UV–spectroscopy, J. Hazard. Mater. B. 122 (2005) 147–153.
[12] W. Zhang, Z. Xu, B. Pan, C. Hong, K. Jia, P. Jiang, Q. Zhang, B. Pan, Equilibrium and heat of adsorption of diethyl phthalate on heterogeneous adsorbents, J. Colloid Interface Sci. 325 (2008) 41–47.
[13] N. Adhoum, L. Monser, Removal of phthalate on modified activated carbon: Application to the treatment of industrial wastewater, Sep. Purif. Technol. 38 (2004) 233–239.
[14] M. Julinová, R. Slavík, Removal of phthalates from aqueous solution by different adsorbents: A short review, J. Environ. Manage. 94 (2012) 13–24.
[15] S. Venkata Mohan, S. Shailaja, M. Rama Krishna, P.N. Sarma, Adsorptive removal of phthalate ester (Diethyl phthalate) from aqueous phase by activated carbon: A kinetic study, Polym. Test. 146(1–2) (2007) 278–282.
[16] E. Tümay Özer, B. Osman, A. Kara, N. Beşirli, Ş. Gücer, H. Sözeri, Removal of diethyl phthalate from aqueous phase using magnetic poly(EGDMA–VP) beads, J. Hazard. Mater. 229–230 (2012) 20–28.
[17] B. Osman, E. Tümay Özer, A. Kara, Ş. Güçer, N. Beşirli, Assesment of dimethyl phthalate removal from aqueous phase using barium hexaferrite containing magnetic beads, J. Colloid Interface Sci. 378 (2012) 167–174.
[18] B. Osman, E. Tümay Özer, E. Demirbel, Ş. Güçer, N. Beşirli, Synthesis and characterization of L-tryptophan containing microbeads for removal of dimethyl phthalate from aqueous phase, Sep. Purif. Technol. 109 (2013) 40–47.
[19] B. Osman, E. Tümay Özer, N. Beşirli, Ş. Güçer, Development and application of a solid phase extraction method for the determination of phthalates in artificial saliva using new synthesised microspheres, Polym. Test. 32(4) (2013) 810–818.
[20] E. Tümay Özer, B. Osman, A. Kara, E. Demirbel, N. Beşirli, Ş. Güçer, Diethyl phthalate removal from aqueous phase using poly(EGDMA-MATrp) beads: Kinetic, isothermal and thermodynamic studies, Cem. Concr. Res. 36(13) (2015) 1698–1706.
[21] J.P. Rao, K.E. Geckeler, Polymer nanoparticles: Preparation techniques andsize-control parameters, Prog. Polym. Sci. 36 (2011) 887–913.
[22] L. Sun, J. Dai, G.L. Baker, M.L. Bruening, High-capacity, protein-binding membranes based on polymer brushes grown in porous substrates, Chem. Mater. 18 (2006) 4033–4039.
[23] J. Dai, Z. Bao, L. Sun, S.U. Hong, G.L. Baker, M.L. Bruening, High-capacity binding of proteins by poly (acrylic acid) brushes and their derivatives, Langmuir 22 (2006) 4274–4281.
[24] X. Wu, H. Hong, X. Liu, W. Guan, L. Meng, Y. Ye, Y. Ma, Graphene dispersive solid-phase extraction of phthalate acid esters from environmental water, Sci. Total Environ. 444 (2013) 224–230.
[25] L. Yin, Y. Lin, L. Jia, Graphene oxide functionalized magnetic nanoparticles as adsorbents for removal of phthalate esters, Microchim. Acta 181 (2014) 957–965.
[26] X. Cao, Q. Kong, R. Cai, K. Zhu, X. Ye, J. Chen, W. Mo, J. Wang, Solid-phase extraction based on chloromethylated polystyrene magnetic nanospheres followed by gas chromatography with mass spectrometry to determine phthalate esters in beverages, J. Sep. Sci. 37 (2014) 3677–3683.
[27] Y.B. Luo, Q.W. Yu, B.F. Yuan, Y.Q. Feng, Fast microextraction of phthalate acid esters from beverage, environmental water and perfume samples by magnetic multi-walled carbon nanotubes, Talanta 90 (2012) 123–131.
[28] C.Y. Chen, Y.C. Chung, Removal of phthalate esters from aqueous solutions by chitosan bead, J. Environ. Sci. Health Part A 41 (2006) 235–248.
[29] C.Y. Chen, Y.C. Chung, Removal of phthalate esters from aqueous solution by molybdate impregnated chitosan beads, Environ. Eng. Sci. 24 (2007) 834–841.
[30] C.Y. Chen, C.C. Chen, Y.C. Chung, Removal of phthalate esters by α-cyclodextrin-linked chitosan bead, Bioresour. Technol. 98 (2007) 2578–2583.
[31] Q. Wu, M. Liu, X. Ma, W. Wang, C. Wang, X. Zang, Z. Wang, Extraction of phthalate esters from water and beverages using a graphene-based magnetic nanocomposite prior to their determination by HPLC, Microchim. Acta. 177 (2012) 23–30.

[32] Q. Xu, X. Yin, S. Wu, M. Wang, Z. Wen, Z. Gu, Determination of phthalate esters in water samples using Nylon6 nanofibers mat-based solid-phase extraction coupled to liquid chromatography, Microchim. Acta 168 (2010) 267–275.
[33] N.M. Agyei, C.A. Strydom, J.H. Potgieter, An investigation of phosphate ion adsorption from aqueous solution by fly ash and slag, Cem. Concr. Res. 30(5) (2000) 823–826.
[34] Y.S. Ho, G. Mckay, Competitive sorption of copper and nickel ions from aqueous solution using peat, Adv. Colloid Interface Sci. 5(4) (1999) 409–417.
[35] S. Baup, C.D. JaffreWolbert, A. Laplanche, Adsorption of pesticides onto granular activated carbon: Determination of surface diffusivities using simple batch experiments, Adsorption 6(3) (2000) 219–228.
[36] K.Y. Foo, B.H. Hameed, Insights into the modeling of adsorption isotherm systems, Chem. Eng. J. 156(1) (2010) 2–10.
[37] M. Ahmaruzzaman, Adsorption of phenolic compounds on low-cost adsorbents: A review, Adv. Colloid Interface Sci. 143(1–2) (2008) 48–67.
[38] J. Zeldowitsch, Adsorption site energy distribution, Acta Phys. Chim. URSS. 1 (1934) 961–973.